Article

High-Temperature Chemical Stability of Cr(III) Oxide Refractories in the Presence of Calcium Aluminate Cement

Tengteng Xu [1,2]**, Yibiao Xu** [1,2,]*****, Ning Liao** [1,2]**, Yawei Li** [1,2,]***** **and Mithun Nath** [1,2,]*****

[1] The State Key Laboratory of Refractories and Metallurgy, Wuhan University of Science and Technology, Wuhan 430081, China; xutengteng1992@163.com (T.X.); liaoning@wust.edu.cn (N.L.)

[2] National-Provincial Joint Engineering Research Center of High Temperature Materials and Lining Technology, Wuhan University of Science and Technology, Wuhan 430081, China

***** Correspondence: xuyibiao@wust.edu.cn (Y.X.); liyawei@wust.edu.cn (Y.L.); mithunnath@wust.edu.cn (M.N.)

Abstract: Al_2O_3-CaO-Cr_2O_3 castables are used in various furnaces due to excellent corrosion resistance and sufficient early strength, but toxic Cr(VI) generation during service remains a concern. Here, we investigated the relative reactivity of analogous Cr(III) phases such as Cr_2O_3, $(Al_{1-x}Cr_x)_2O_3$ and in situ Cr(III) solid solution with the calcium aluminate cement under an oxidizing atmosphere at various temperatures. The aim is to comprehend the relative Cr(VI) generation in the low-cement castables (Al_2O_3-CaO-Cr_2O_3-O_2 system) and achieve an environment-friendly application. The solid-state reactions and Cr(VI) formation were investigated using powder XRD, SEM, and leaching tests. Compared to Cr_2O_3, the stability of $(Al_{1-x}Cr_x)_2O_3$ against CAC was much higher, which improved gradually with the concentration of Al_2O_3 in $(Al_{1-x}Cr_x)_2O_3$. The substitution of Cr_2O_3 with $(Al_{1-x}Cr_x)_2O_3$ in the Al_2O_3-CaO-Cr_2O_3 castables could completely inhibit the formation of Cr(VI) compound $CaCrO_4$ at 500–1100 °C and could drastically suppress $Ca_4Al_6CrO_{16}$ generation at 900 to 1300 °C. The Cr(VI) reduction amounting up to 98.1% could be achieved by replacing Cr_2O_3 with $(Al_{1-x}Cr_x)_2O_3$ solid solution. However, in situ stabilized Cr(III) phases as a mixture of $(Al_{1-x}Cr_x)_2O_3$ and $Ca(Al_{12-x}Cr_x)O_{19}$ solid solution hardly reveal any reoxidation. Moreover, the CA_6 was much more stable than CA and CA_2, and it did not participate in any chemical reaction with $(Al_{1-x}Cr_x)_2O_3$ solid solution.

Keywords: Al_2O_3-CaO-Cr_2O_3-O_2 system; $(Al_{1-x}Cr_x)_2O_3$; $Ca(Al_{12-x}Cr_x)O_{19}$; Cr(VI) compounds; leaching test

1. Introduction

Cr_2O_3-containing refractories possess remarkable corrosion resistance due to their extremely low solubility and high chemical stability against molten slag. Therefore, they are widely used as lining materials in incinerators, gasifiers, glass furnaces, non-ferrous smelting, etc. [1–6]. In addition, refractories as castables have become a popular choice in recent decades because of the energy-saving manufacturing process, convenient for installation and repair works, where binders' chemistry plays a crucial role [7–9]. Calcium alumina cement (CAC) binders are the most widely used since they exhibit fast setting and strength development, stable thermo-mechanical behaviour, and resistance to slag attack [10]. However, Cr_2O_3 can oxidize into toxic Cr(VI) products at high temperatures upon reaction with alkali or alkaline earth metals/oxides/compounds under an oxidizing atmosphere [11–13]. The Cr(VI) compounds pose a severe threat to humans and the environment since they are toxic, carcinogenic, highly soluble in water, and quickly enter the food cycle [14]. Therefore, it is of significant environmental and practical significance to inhibit the generation of Cr(VI) when applying Al_2O_3-CaO-Cr_2O_3 castables as lining materials.

The Al_2O_3-CaO-Cr_2O_3 system was not investigated in detail earlier though numerous Cr(VI) reduction techniques were described for other applications [15–17]. Generally, Cr(VI) formation was closely related to the atmosphere and basicity of other components in the

Cr_2O_3-containing materials [18,19]. For the Cr_2O_3-containing refractory linings, since the operating conditions and service atmosphere in a given furnace can hardly be changed in practical production, most related work has focused on Cr(VI) minimization using some additives at high temperatures. The acidic components such as SiO_2, TiO_2, Fe_2O_3, and P_2O_5 can effectively suppress the Cr(III) oxidation during thermal treatment of Cr_2O_3-containing refractories [19–22]. However, these oxide additives usually result in low melting point phases in the matrix, deteriorating either the thermo-mechanical properties or the slag corrosion resistance [23,24]. Previous research indicated that incorporating chromium into solid solution phases can reduce the risk of Cr(VI) formation in the Cr_2O_3-containing materials [25–27]. For example, the investigation of the Al_2O_3-Cr_2O_3-CaO-MgO pure system confirmed that composite spinel $Mg(Al,Cr)_2O_4$ could co-exist with CA_2, where chromium existed in +3 state [25,27]. Again, Wu et al. [28] studied the effect of temperature on Cr(VI) formation in a pure $(Al,Cr)_2O_3$ system with CAC in air atmosphere, where $(Al_{1-x}Cr_x)_2O_3$ was found to be chemically stable against CAC up to 1100 °C, beyond which $Ca_4Al_6CrO_{16}$ (hauyne) phase predominantly start from.

Nath et al. investigated the phase evolution of the Al_2O_3-CaO-Cr_2O_3 refractories castables after treatment at various temperatures, where CaO from cement facilitated the conversion of Cr(III) into Cr(VI) [29]. The main phase of CAC (CA and CA_2) react with Cr_2O_3 in the air to produce $CaCrO_4$ and $Ca_4Al_6CrO_{16}$ at mid-temperature (700–1100 °C). At the same time, nearly all the Cr_2O_3 would convert into $(Al_{1-x}Cr_x)_2O_3$ (0 < x < 1) and $Ca(Al,Cr)_{12}O_{19}$ solid solution at 1500 °C, which leads to a significant decrease of Cr(VI) compounds amounts [20,29]. Thus, $(Al_{1-x}Cr_x)_2O_3$ solid solutions having high refractoriness and good chemical stability could be better performing materials with better mechanical properties and slag corrosion resistance [30–33]. Based on the above research, it can be inferred that substituting Cr_2O_3 with $(Al_{1-x}Cr_x)_2O_3$ solid solution as a starting component in the Al_2O_3-CaO-Cr_2O_3 castables could be a feasible way to inhibit the formation of Cr(VI) at various temperatures, especially at mid-temperature (700–1100 °C), without compromising other properties. However, systematic work relating to the effect of $(Al_{1-x}Cr_x)_2O_3$ solid solution on Cr(VI) formation in Al_2O_3-CaO-Cr_2O_3 refractory castables is rare.

The present work aims to inhibit the formation of Cr(VI) compounds in Al_2O_3-CaO-Cr_2O_3 castables by substituting Cr_2O_3 with $(Al_{1-x}Cr_x)_2O_3$ solid solution as starting chromium-containing constituent. Firstly, $(Al_{1-x}Cr_x)_2O_3$ solid solutions were pre-synthesized at 1300 to 1650 °C. Secondly, Al_2O_3-CaO-Cr_2O_3 castables with the pre-synthesized $(Al_{1-x}Cr_x)_2O_3$ solid solution were fabricated and treated at the temperature range of 300–1500 °C in the air since castables would be put to use without firing and a temperature gradient occurs in any furnace linings in actual practice. The phase evolution and Cr(VI) generation of the Al_2O_3-CaO-Cr_2O_3 castables with temperature and the corresponding mechanism were studied using XRD and related software, SEM, and leaching tests. Furthermore, since the $(Al_{1-x}Cr_x)_2O_3$ and $Ca(Al,Cr)_{12}O_{19}$ could be formed in the Al_2O_3-CaO-Cr_2O_3 castables at high temperature [20], castables with Cr_2O_3 were pre-heated at 1500 °C to produce the in situ formed $(Al_{1-x}Cr_x)_2O_3$, whose effect on the Cr(VI) formation for the castables at various temperature was also evaluated.

2. Materials and Methods

Tabular alumina (Al_2O_3) of various size fractions, 5–3 mm, 3–1 mm, 1–0 mm, and $\leq$0.045 mm, were procured from Zhejiang Zili Alumina Materials Technology Co., Ltd., Shangyu, China. Reactive α-alumina fines of size fraction $\leq$ 0.005 mm were purchased from Kaifeng Tenai Co., Ltd., Kaifeng, China. Industrial-grade fused chromium oxide (Cr_2O_3) (size $\leq$ 0.074 mm) was obtained from Luoyang Yuda Refractories Co., Ltd., Luoyang, China. The hydraulic calcium aluminate cement binder, Secar 71 (CA and CA_2 phases), was procured from Imerys Aluminates, Tianjin, China. An organic deflocculant, FS 65 (Wuhan Sanndar Chemical Co., Ltd., Wuhan, China), was used as the dispersant. The detailed chemical composition of raw materials is shown in Table 1.

Table 1. The chemical composition of raw materials (wt%).

Raw Materials	SiO_2	Al_2O_3	CaO	Fe_2O_3	MgO	Na_2O	K_2O	Cr_2O_3
Tabular alumina	0.08	99.30	-	0.02	-	0.28	-	-
Reactive α-alumina	0.28	98.87	0.07	0.13	0.12	0.10	0.005	-
Fused chromium oxide	0.82	0.59	0.38	0.73	0.27	0.14	0.01	94.02
Calcium aluminate cement	0.40	70.6	28.4	0.20	-	-	-	-

Cr_2O_3 and Al_2O_3 fine powders with a mass ratio of 8:17 were dry-mixed, pressed into pellets, and then treated at 1300, 1600, and 1650 °C for 3 h in the air to obtain the mixture of Al_2O_3, Cr_2O_3 and $(Al_{1-x}Cr_x)_2O_3$ solid solution and pre-synthesized $(Al_{1-x}Cr_x)_2O_3$ solid solution. Thus, obtained pellets were then pulverized to 200-mesh powders before adding them into the castables. The specimen with Cr_2O_3 and Al_2O_3 powders as initial raw materials was labelled as R, while specimens with $(Al_{1-x}Cr_x)_2O_3$ solid solution pre-synthesized at 1300 °C, 1600 °C, and 1650 °C were designated as S13, S16, and S165, respectively. Specimen R was pre-heated at 1500 °C for 3h (labelled as F15) to produce the in situ formed $(Al_{1-x}Cr_x)_2O_3$, whose effect on the Cr(VI) formation in the castables at various temperatures was also evaluated then. The castables were formulated based on the Andreasen distribution coefficient (q) value of 0.31, and the specific formulation is shown in Table 2. Each batch was dry-mixed for 3 min in a Hobart mixer followed by wet-mixing (4.0 wt% water, 25 °C) for further 3 min, and then castables were moulded in a vibrating table (1 min) into bars of size 160 mm × 40 mm × 40 mm at room temperature. All specimens were cured at 25 °C and 75% ± 5% relative humidity for 24 h in a standard cement maintainer and dried at 110 °C for 24 h in an electric air oven after demoulding. Dried specimens R, S13, S16, S165, and specimen F15 were finally heated in the temperature range of 300–1500 °C for 3h at peak temperature in air.

Table 2. The formulation of fine powders undergoing reaction within castables (30wt% of total).

Code	Aggregates Al_2O_3 (wt%)	Fine Powders (wt%)				Pre-Treatment Temperature (°C)
		Al_2O_3	Cr_2O_3	CAC	$(Al_{1-x},Cr_x)_2O_3$	
R	70	17	8	5	-	-
F15	70	17	8	5	-	In situ treated at 1500
S13	70	-	-	5	25	$(Al_{1-x},Cr_x)_2O_3$ made at 1300
S16	70	-	-	5	25	$(Al_{1-x},Cr_x)_2O_3$ made at 1600
S165	70	-	-	5	25	$(Al_{1-x},Cr_x)_2O_3$ made at 1650

Note: 0.1 wt% additional organic dispersant was added to each formulation to make the castables. CAC designates calcium aluminate cement (Here, a commercial Secar 71 cement was used). Each batch contains 8 wt% of Cr_2O_3.

To figure out relative oxidation, the mechanisms of the Cr(VI) generation in the castables and the corresponding chemical reactions, fine powders of CAC and CA_6 were mixed with Cr_2O_3 and pre-synthesized $(Al_{1-x}Cr_x)_2O_3$ (Table 3). Then, the mixed powders were pressed into Φ20 mm × 20 mm cylindrical specimens under a pressure of 50 MPa. After being treated at 900 °C and 1300 °C for 3 h in the air atmosphere, the phase compositions and microstructures of the specimens were analyzed by XRD and SEM, respectively.

Table 3. The formulation of cylindrical specimens (wt%).

Specimens	CAC	CA_6	Cr_2O_3	$(Al_{1-x},Cr_x)_2O_3$
C-C	50		50	
C-S	50			50
CH-C		50	50	
CH-S		50		50

Note: CAC (Secar 71) contains mixture of $CaAl_2O_4$ (63%) and $Ca_2Al_4O_7$ (35%), $CA_6 = CaAl_{12}O_{19}$.

The crystalline phase compositions were identified by X-ray diffraction (XRD) patterns using a X'Pert Pro diffractometer (PANalytical, Almelo, Netherlands) (Copper Kα radiation (λ = 1.5418 Å) at 40 kV/40 mA, step size 0.02 over a 2θ range of 5–90°) and analyzed by

the software of X'pert Pro High Score (Philips, Almelo, Netherlands). Lattice parameters were calculated using X'pert Pro High Score (Philips, Almelo, Netherlands) and Celref 2.0 software. Microstructure morphology was analyzed by scanning electron microscopy (SEM, Nova 400 Nano-SEM, FEI Company, Hillsboro, OR, USA) equipped with energy dispersive spectroscopy (EDS, Oxford, High Wycombe, UK).

Cr(VI) leachability was evaluated using the leaching test according to TRGS 613 standard procedure, which is suitable for determining water-soluble Cr(VI) compounds in cement and products containing cement. Leaching specimens were prepared by crushing and grinding thoroughly before passing through a 200-mesh sieve ($\leq$74 μm). Fine samples were stirred with deionized water as a leaching solution using a magnetic stirrer at a speed of 300 rpm for 15 min (at room temperature) with a solid–liquid ratio of 1:20. Then, leachates were obtained through a 0.45-μm membrane filter with a glass fibre by vacuum. The Cr(VI) concentration in the leachates was determined using a colorimetric method. The Cr(VI) can react in acid condition with the 1,5-diphenylcarbazide (DPC) to form 1,5-diphenylcarbazone, a red complex (0.02–0.2 mg/L chrome). Then, the absorbance of the leachates after the DPC method was recorded at 540 nm, using a 722 Vis spectrophotometer (Jinghua Instruments, Shanghai, China).

3. Results and Discussion

3.1. Pre-Synthesis of $(Al_{1-x}Cr_x)_2O_3$ Powders

The pre-synthesized powders of the $(Al_{1-x}Cr_x)_2O_3$ solid solution at different temperatures are observed by XRD (Figure 1). It could be found that both corundum and eskolaite existed as separate phases after dry mixing at 25 °C. After treated at 1300 °C, the eskolaite disappeared with a noticeable reduction of the peak intensity of corundum, while a new phase identified as $(Al_{1-x}Cr_x)_2O_3$ solid solution was generated. With the increase in the heat treatment temperature, the peak intensity of corundum reduced gradually until disappearance at 1650 °C, while the peak intensity of $(Al_{1-x}Cr_x)_2O_3$ solid solution increased steadily. After treated at temperatures up to 1650 °C, only the $(Al_{1-x}Cr_x)_2O_3$ solid solution could be detected in the specimens. So, it could be inferred that we have added the $(Al_{1-x}Cr_x)_2O_3$ solid solution with the remnant of corundum and eskolaite (sample S13 and S16), while that of S165 is a complete $(Al_{1-x}Cr_x)_2O_3$ solid solution. In addition, the lattice parameters of the $(Al_{1-x}Cr_x)_2O_3$ solid solution were calculated in comparison with Al_2O_3 (reference code: JCPDS 01-081-2266, $a = b = 4.7569$ Å and $c = 12.9830$ Å) and Cr_2O_3 (reference code: JCPDS 00-038-1479, $a = b = 4.9540$ Å and $c = 13.5842$ Å). Since Al_2O_3 has smaller lattice parameters than Cr_2O_3, the $(Al_{1-x}Cr_x)_2O_3$ solid solution reveals smaller lattice parameters than Cr_2O_3. With the increasing temperature, the $(Al_{1-x}Cr_x)_2O_3$ solid solution showed decreasing lattice parameters as more Al_2O_3 dissolution is expected at higher temperatures. For example, the lattice parameter $a = b = 4.8607$ Å at 1300 °C (for sample S13) decreased to $a = b = 4.8291$ Å at 1600 °C (for sample S16).

3.2. Cr(VI) Leachability

The Cr(VI) concentration in Al_2O_3-CaO-Cr_2O_3 castables treated at various temperatures was evaluated by leaching test according to the TRGS 613 standard procedure (Figure 2). The details of Cr(VI) reduction compared to the reference specimen R is presented in Table 4. With the addition of the pre-synthesized $(Al_{1-x}Cr_x)_2O_3$ solid solution, a noticeable decrease in the Cr(VI) concentration was observed. The specimens with $(Al_{1-x},Cr_x)_2O_3$ pre-synthesized at higher temperature exhibited relatively lower Cr(VI) concentrations at the same heat treatment temperature (exception for specimen S165 at 1300 and 1500 °C). For example, at 700 °C, the total amount of Cr(VI) reduced drastically from 1233.2 mg/kg in specimen R (without $(Al_{1-x}Cr_x)_2O_3$) to 223.7 mg/kg in specimen S13 (a reduction of 81.9%), and reduced further to 24.0 mg/kg in specimen S165 (a decrease of 98.1%). However, at 1300 °C, specimen S165 exhibited an even higher Cr(VI) concentration than the reference specimen. Moreover, the temperature corresponding to the maximum Cr(VI) concentration shifted from 900 °C for R to 1100 °C for the pre-

synthesized $(Al_{1-x}Cr_x)_2O_3$. The specimen F15, pre-heated at 1500 °C, exhibited extremely low Cr(VI) concentration at all heat treatment temperatures studied. It was concluded that the chromium would present as Cr(III) together within the solid solution of $(Al_{1-x}Cr_x)_2O_3$ and $Ca(Al,Cr)_{12}O_{19}$ after the pre-heating treatment at 1500 °C [20]. Therefore, it is plausible that the reoxidation of these stable solid solution phases did not occur. Although the mid-temperature (700–1100 °C) was favourable for Cr(VI) formation, the total amount of Cr(VI) in F15 was still only 13.0-17.3 mg/kg (a decrease of ~98.9–99.1% compared to specimen R). These values are below the allowable Cr(VI) limit of the Environmental Protection Agency (EPA), United States (5 mg/L is equivalent to 100 mg/kg) [34].
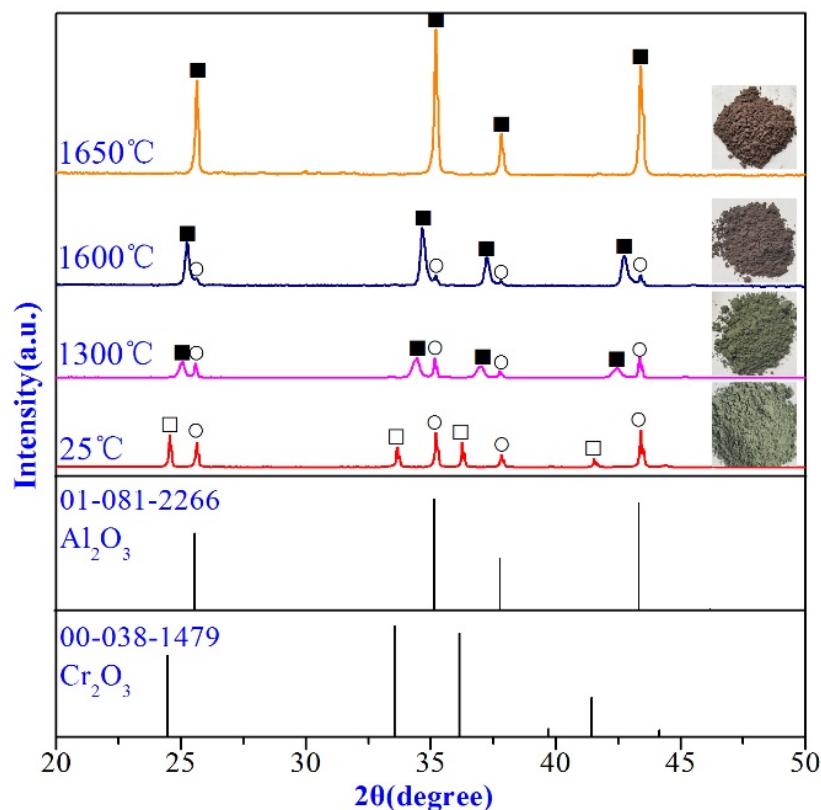

Figure 1. XRD pattern of $(Al_{1-x}Cr_x)_2O_3$ solid solution pre-synthesized at different temperatures. ○-Corundum (Al_2O_3), ■-$(Al_{1-x},Cr_x)_2O_3$ solid solution, □-Eskolaite (Cr_2O_3).

Table 4. Relative Cr(VI) reduction (%) of specimens compared to R at different temperatures.

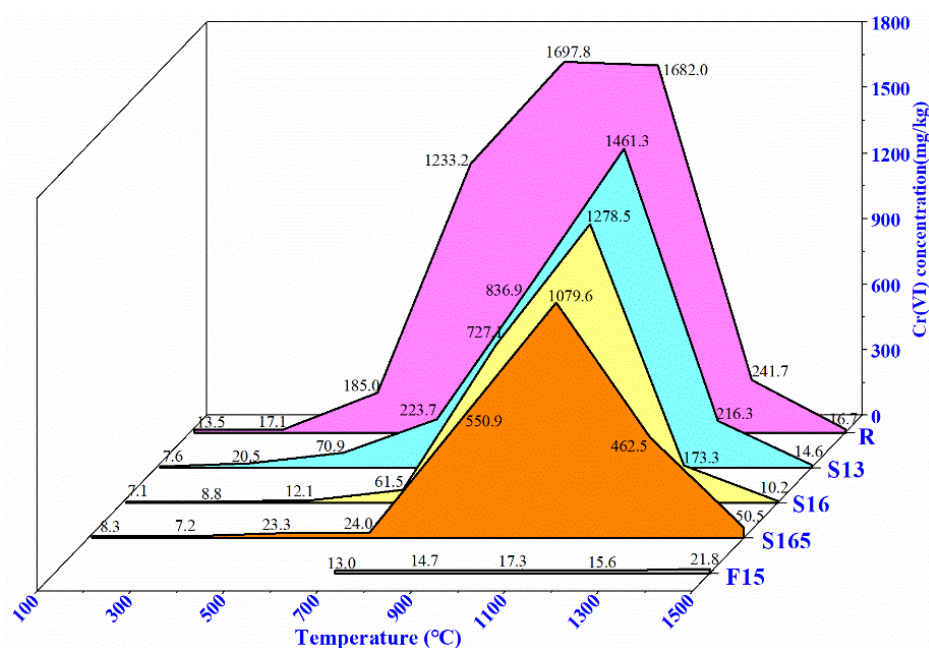| Specimens	Temperature (°C)							
	110	300	500	700	900	1100	1300	1500
S13	43.7	−19.5	61.7	81.9	16.1	21.2	10.5	12.6
S16	47.4	48.6	93.4	95.0	57.2	24.0	28.0	38.7
S165	38.5	58.0	87.4	98.1	67.6	35.8	−91.4	−202.4
F15	-	-	-	98.9	99.1	99.0	93.5	−30.8

Figure 2. Cr(VI) concentration as a function of temperature in the Al_2O_3-CaO-Cr_2O_3 castables.

3.3. Phase Evolution of the Castables

To study the effect of the pre-synthesized $(Al_{1-x}Cr_x)_2O_3$ solid solution on the phase evolution of the castables, phase compositions of the specimens treated at 110–1500 °C were analyzed (Figure 3). In all samples, the main phase corundum and the $NaAl_{11}O_{17}$ impurity could be detected at all temperatures, and hydrate phase C_3AH_6 was generated at 110 °C but then disappeared at 300 °C due to dehydration. For specimen R, the $CaCrO_4$ phase could be detected at 300 °C, whose peak intensity increased with the increase in temperature from 300 °C to 900 °C but then decreased with further increasing temperature until disappearance at 1300 °C. The $Ca_4Al_6CrO_{16}$ was generated at 900 °C, whose peak intensity reached a maximum at 1100 °C but dropped down with further increasing temperature until disappearance at 1500 °C. Moreover, eskolaite existing in the range of 110 °C to 1100 °C reduced in peak intensity with temperature and disappeared at 1300 °C, while the $(Al_{1-x}Cr_x)_2O_3$ solid solution and $CaAl_{12}O_{19}$ increased in peak intensity after generating at 1100 °C and 1300 °C, respectively. However, for specimens S13, S16, and S165, no $CaCrO_4$ phase was detected at 300–1100 °C, indicating chromium that in the $(Al_{1-x}Cr_x)_2O_3$, the CAC in this temperature range would not oxidize the solid solution. At 900–1300 °C, although the $Ca_4Al_6CrO_{16}$ phase was still formed in these specimens with pre-synthesized $(Al_{1-x}Cr_x)_2O_3$, the peak intensity of Cr(VI) compound was much lower compared with sample R. The peak intensity of the $Ca_4Al_6CrO_{16}$ phase reached the maximum at 1100 °C in Al_2O_3-CaO-Cr_2O_3 castables, and therefore, the highest Cr(VI) concentration for the specimens with pre-synthesized $(Al_{1-x}Cr_x)_2O_3$ were detected at 1100 °C (Figure 3b). In general, the substitution of Cr_2O_3 with $(Al_{1-x}Cr_x)_2O_3$ in the Al_2O_3-CaO-Cr_2O_3 castables can almost completely restrict the formation of $CaCrO_4$ compounds at 300–1100 °C and effectively lower the Cr(VI) compound $Ca_4Al_6CrO_{16}$ formation at 900–1300 °C, which was following the results of Cr(VI) leachability shown in Figure 2. After being treated at 1500 °C, only the corundum (with $NaAl_{11}O_{17}$ impurity), the $(Al_{1-x}Cr_x)_2O_3$ solid solution, and the CA_6 phases were found in specimens R, S13, S16, and S165. The enlarged XRD patterns of the castables (Figure 3c) indicated that samples with $(Al_{1-x}Cr_x)_2O_3$ pre-synthesized at higher temperature exhibited relative lower peak intensity of the CA_6 phase after being treated at 1300 °C. In addition, specimen F15, which had the same phase compositions as the other four specimens treated at 1500 °C, showed hardly any phase changes with the subsequent heat treatment temperature.
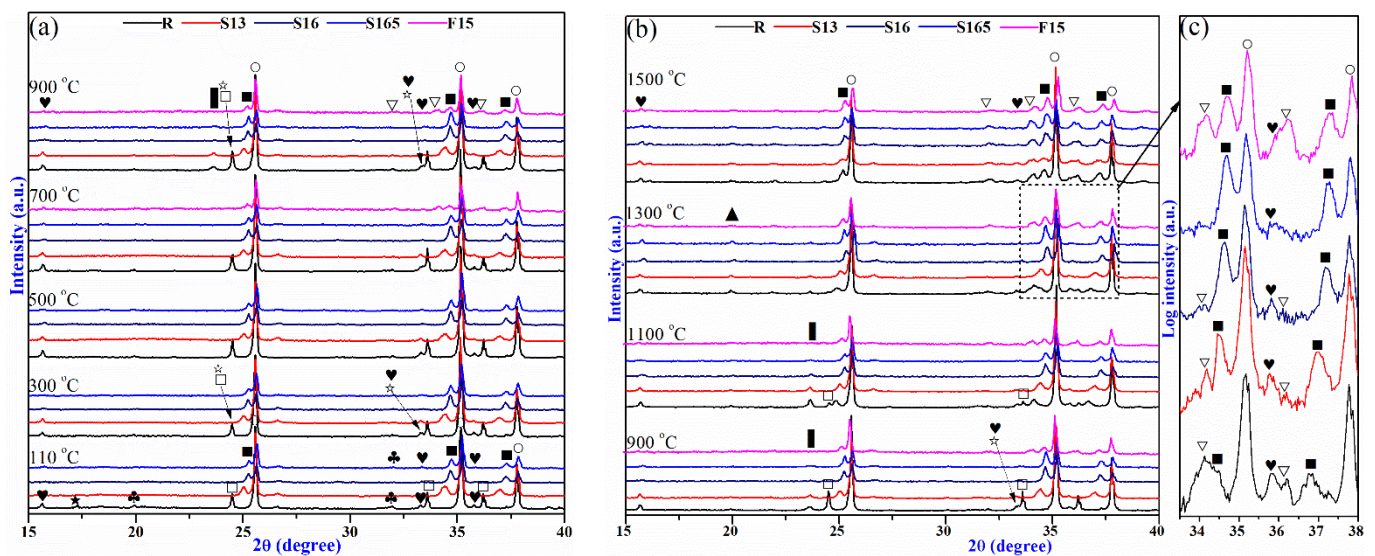
Figure 3. XRD patterns of Al_2O_3-CaO-Cr_2O_3 castables, (**a**) 110–900 °C, (**b**) 900–1500 °C, (**c**) 1300 °C. ○—Corundum (Al_2O_3), ■—(Al_{1-x},Cr_x)$_2O_3$ solid solution, □—Eskolaite (Cr_2O_3), ☆—$CaCrO_4$, ❚—Hauyne ($Ca_4Al_6CrO_{16}$), ▽—CA_6 ($CaAl_{12}O_{19}$), ♥—$NaAl_{11}O_{17}$, ♣—C_3AH_6 ($Ca_3Al_2(OH)_{12}$).

3.4. Reaction Mechanism

The above results demonstrated that in the Al_2O_3-CaO-Cr_2O_3 castables, chromium and calcium would exist in the state of Cr_2O_3/($Al_{1-x}Cr_x$)$_2O_3$, and CAC/CA_6, respectively, which affects the formation and concentration of Cr(VI) compounds $CaCrO_4$ and $Ca_4Al_6CrO_{16}$ at mid-temperature (700–1100 °C). Fine powders of CAC/CA_6 were mixed with Cr_2O_3/($Al_{1-x}Cr_x$)$_2O_3$ (pre-synthetized at 1650 °C) to figure out the mechanisms of the Cr(VI) generation in the castables and the corresponding chemical reactions. Then, the mixed powders were treated at 900 and 1300 °C for 3 h in the air; the XRD patterns and SEM microstructure are summarized in Figures 4 and 5, respectively. The plausible chemical reaction equations discussed below in various samples heated at 900 °C and 1300 °C are listed in Table 5. In addition, the qualitative EDS spot analysis (atomic%) was shown in Table 6, corresponding to the fractured surface in Figure 5. Needless to mention that the uneven surface of the specimen would only reveal the non-stoichiometric composition to identify the different phases associated with different morphology.

Table 5. Chemical reaction equations in cylindrical specimens.

Specimens	900 °C	1300 °C
C-C	(1)	(3) (4) (5)
C-S	(2)	(2)
CH-C	-	(5) (6)
CH-S	-	-

$$4CaAl_2O_4 + 2Cr_2O_3 + 3O_2 \rightarrow 4CaCrO_4 + 4Al_2O_3 \qquad (1)$$
$$16CaAl_2O_4 + y(Al_{1-x},Crx)_2O_3 + 3O_2 \rightarrow 4Ca_4Al_6CrO_{16} + (y + 2)Al_2O_3 \qquad (2)$$
$$16CaAl_2O_4 + 2Cr_2O_3 + 3O_2 \rightarrow 4Ca_4Al_6CrO_{16} + 4Al_2O_3 \qquad (3)$$
$$16CaAl_4O_7 + 2Cr_2O_3 + 3O_2 \rightarrow 4Ca_4Al_6CrO_{16} + 20Al_2O_3 \qquad (4)$$
$$(1 - x)Al_2O_3 + xCr_2O_3 \rightarrow (Al_{1-x},Crx)_2O_3 \qquad (5)$$
$$16CaAl_{12}O_{19} + 2Cr_2O_3 + 3O_2 \rightarrow 4Ca_4Al_6CrO_{16} + 84Al_2O_3 \qquad (6)$$
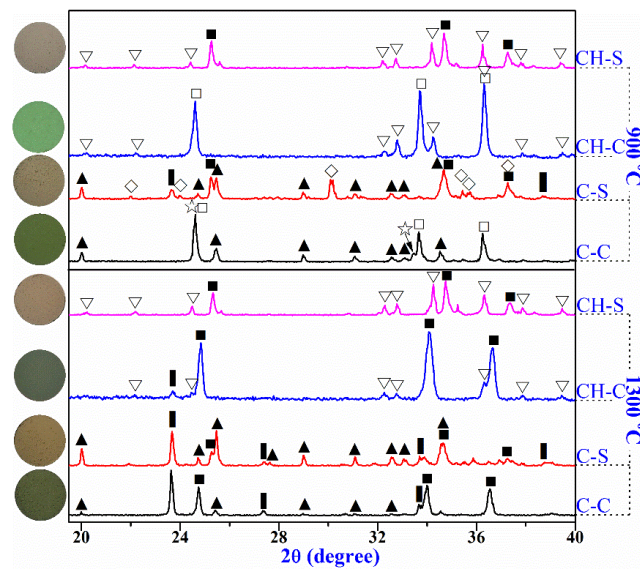
Figure 4. XRD pattern and corresponding images of cylindrical specimens heated at 900 °C and 1300 °C. ■—$(Al_{1-x},Cr_x)_2O_3$ solid solution. □—Eskolaite (Cr_2O_3), ☆—$CaCrO_4$, ▮—Hauyne ($Ca_4Al_6CrO_{16}$), ▲—CA_2 ($CaAl_4O_7$), ◇—CA ($CaAl_2O_4$), ▽—CA_6 ($CaAl_{12}O_{19}$).
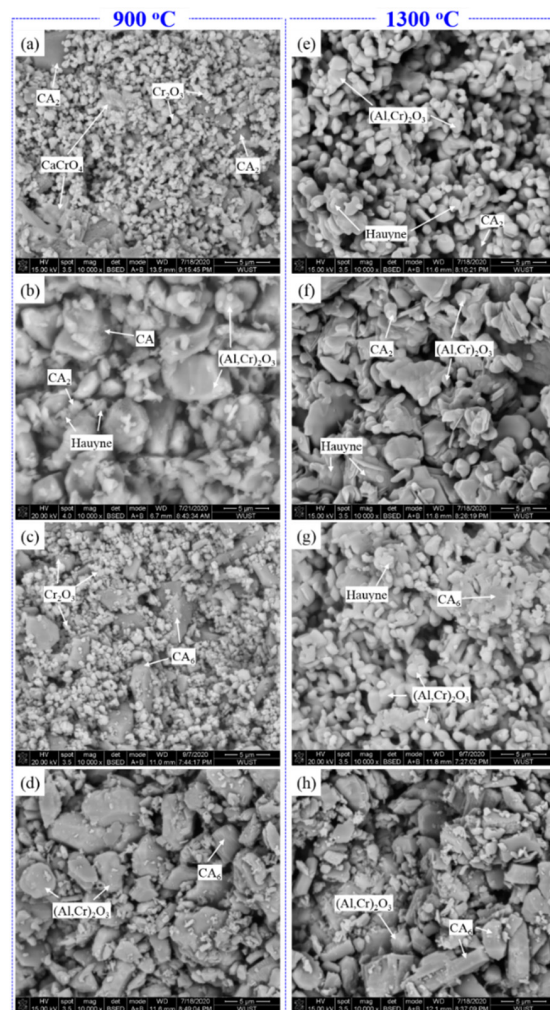

Figure 5. SEM images of cylindrical specimens heated at 900 °C and 1300 °C, (**a**,**e**) C-C; (**b**,**f**) C-S; (**c**,**g**) CH-C; (**d**,**h**) CH-S.

Table 6. Examples of qualitative EDS spot analysis of the samples (atomic%) for identifying various phases in Figure 5.

Phase	Al	Ca	Cr	O
$CaCrO_4$	-	28.36	41.27	30.37
$Ca_6Al_4CrO_{16}$	34.27	18.58	6.34	40.82
$CaAl_2O_4$	40.39	16.94	-	42.68
$CaAl_4O_7$	49.87	4.13	-	46.00
$(Al,Cr)_2O_3$	48.68	-	15.27	36.05

After being treated at 900 °C, the CA phase disappeared in specimen C-C with the formation of many granular $CaCrO_4$ grains (Figure 5a) via reaction 1. However, the sample C-S was still composed of the initial main phases (CA, CA_2, and $(Al_{1-x}Cr_x)_2O_3$) (Figure 5b) in addition to forming minute amounts of $Ca_4Al_6CrO_{16}$ (reaction 2). As the heat treatment temperature increased to 1300 °C, plenty of chrome-hauyne and $(Al_{1-x}Cr_x)_2O_3$ solid solution (Figure 5e) were generated in specimen C-C (via reactions 3–5), accompanied by the disappearance of CA and significant reduction in CA_2 phase, while specimen C-S possessed relative lower peak intensity of $Ca_4Al_6CrO_{16}$ although it had similar phases as C-C. Combining the observations of Cr(VI) in Figure 2, with the phase evolution results (Figures 3 and 4), it can be deduced that compared with Cr_2O_3, the $(Al_{1-x}Cr_x)_2O_3$ solid solution was more stable that would not form $CaCrO_4$ and could effectively hinder the $Ca_4Al_6CrO_{16}$ formation when contacted with CAC. Therefore, the substitution of Cr_2O_3 with $(Al_{1-x}Cr_x)_2O_3$ can effectively lower the Cr(VI) concentration of the castables after being treated at various temperatures (Figure 2). Furthermore, the castables with $(Al_{1-x}Cr_x)_2O_3$ pre-synthesized at higher temperature exhibited lower Cr(VI) concentration, implying that the stability of the $(Al_{1-x}Cr_x)_2O_3$ improved gradually with the Al_2O_3 proportion in the solid solution. In addition, in comparison with the CA_2 phase, CA was more likely to react with $Cr_2O_3/(Al_{1-x}Cr_x)_2O_3$ resulting in the formation of Cr(VI) compounds.

For specimens CH-C, no new phases occurred after heat treatment at 900 °C, and only a minuscule amount of chrome-hauyne was generated at 1300 °C (Figure 5g) via Eqs. 6, which also produced Al_2O_3 that subsequently interacted with Cr_2O_3 to develop the $(Al_{1-x}Cr_x)_2O_3$ solid solution via Eqs. 5. It is worth mentioning that no changes in the phase compositions were detected in specimen CH-S after heat treatment at both 900 °C and 1300 °C (Figure 4). These observations demonstrated that calcium in CA_6 was much more stable than in CA and CA_2, which only caused slight oxidation of Cr_2O_3 and would not take chemical reaction with $(Al_{1-x}Cr_x)_2O_3$ solid solution. Therefore, specimen F15, in which chromium and calcium existed in $(Al_{1-x}Cr_x)_2O_3$ and CA_6, respectively, showed no changes in phase composition and extremely low Cr(VI) concentration at various heat treatment temperatures. In the Al_2O_3-CaO-Cr_2O_3 castables, CA_6 could be generated from the reaction between CAC and Al_2O_3 powders in the matrix at 1300 °C (Figure 4). However, for specimen S165, since no Al_2O_3 existed in the $(Al_{1-x}Cr_x)_2O_3$ powder pre-synthesized at 1650 °C, the calcium would still exist as CA and CA_2 rather than CA_6 at 1300 °C. As a result, specimen S165 possessed an even higher Cr(VI) concentration than the reference specimen R at 1300 °C, suggesting that CA and CA_2 can more easily react with $(Al_{1-x}Cr_x)_2O_3$ to produce $Ca_4Al_6CrO_{16}$ compared with CA_6.

4. Conclusions

In the present work, $(Al_{1-x}Cr_x)_2O_3$ solid solution was pre-synthesized at a different temperatures for the inhibition of the formation of Cr(VI) in Al_2O_3-CaO-Cr_2O_3 castables was systematically investigated. The summarized conclusions are as follows:

(1)   Compared with Cr_2O_3, the stability of the $(Al_{1-x}Cr_x)_2O_3$ solid solution in contact with CAC was much higher. Furthermore, the substitution of Cr_2O_3 with $(Al_{1-x}Cr_x)_2O_3$ in the Al_2O_3-CaO-Cr_2O_3 castables can completely inhibit the midtemperature (300–1100 °C) formation of Cr(VI) compound $CaCrO_4$ and relatively higher temperature Cr(VI) phase $Ca_4Al_6CrO_{16}$ (hauyne) drastically reduced at 900

to 1300 °C. Therefore, replacing Cr_2O_3 with $(Al_{1-x}Cr_x)_2O_3$ can effectively lower the Cr(VI) concentration of the castables after being treated at various temperatures, and a reduction in Cr(VI) amounts up to 98.1% with $(Al_{1-x}Cr_x)_2O_3$ addition could be achieved. Most importantly, Cr(III) present within the in situ $(Al_{1-x}Cr_x)_2O_3$ and $Ca(Al,Cr)_{12}O_{19}$ solid solution phases showed maximum reoxidation resistance and thus need further investigation.

(2) In comparison with the CA_2 phase, CA was more likely to react with $Cr_2O_3/(Al_{1-x}Cr_x)_2O_3$, resulting in Cr(VI) compound formation. Simultaneously, calcium in CA_6 was much more stable than in CA and CA_2, which only caused slight oxidation of Cr_2O_3 and would not undergo a chemical reaction with $(Al_{1-x}Cr_x)_2O_3$ solid solution. Thus, incorporating some Al_2O_3 powders in the matrix of the Al_2O_3-CaO-Cr_2O_3 castables to form CA_6 at a temperature above 1300 °C was also essential for inhibiting Cr(VI) formation when using $(Al_{1-x}Cr_x)_2O_3$ solid solution as a substitute for Cr_2O_3.

References

1. Weinberg, A.V.; Varona, C.; Chaucherie, X.; Goeuriot, D.; Poirier, J. Extending refractory lifetime in rotary kilns for hazardous waste incineration. *Ceram. Int.* **2016**, *42*, 17626–17634. [CrossRef]
2. Kaneko, T.K.; Zhu, J.; Howell, N.; Rozelle, P.; Sridhar, S. The effects of gasification feedstock chemistries on the infiltration of slag into the porous high chromia refractory and their reaction products. *Fuel* **2014**, *115*, 248–263. [CrossRef]
3. Nath, M.; Song, S.; Liu, H.; Li, Y. $CaAl_2Cr_2O_7$: Formation, Synthesis, and Characterization of a New Cr(III) Compound under Air Atmosphere in the Al_2O_3-CaO-Cr_2O_3 System. *Ceram. Int.* **2019**, *45*, 16476–16481. [CrossRef]
4. Nath, M.; Song, S.; Liao, N.; Xu, T.; Liu, H.; Tripathi, H.S.; Li, Y. Co-existence of a Cr^{3+} phase ($CaAl_2Cr_2O_7$) with hydraulic calcium aluminate phases at high-temperature in the Al_2O_3-CaO-Cr_2O_3 system. *Ceram. Int.* **2021**, *47*, 2624–2630. [CrossRef]
5. Perez, I.; Moreno-Ventas, I.; Rios, G. Chemical degradation of magnesia-chromite refractory used in the conversion step of the pyrometallurgical copper-making process: A thermochemical approach. *Ceram. Int.* **2018**, *44*, 18363–18375. [CrossRef]
6. Wu, Y.; Song, S.; Xue, Z.; Nath, M. Formation mechanisms and leachability of hexavalent chromium in Cr_2O_3-containing refractory castables of Electric Arc Furnace cover. *Mater. Metallur. Trans. B* **2019**, *50*, 808–815. [CrossRef]
7. da Luz, A.P.; Braulio, M.A.L.; Pandolfelli, V.C. *Refractory Castable Engineering*; Goller Verlag GmbH: Baden, Germany, 2015.
8. Tomšů, F.; Palčo, S. Refractory monolithics versus shaped refractory products. *Interceram. Int. Ceram. Rev.* **2017**, *66*, 20–23. [CrossRef]
9. Nath, M.; Song, S.; Li, Y.; Xu, Y. Effect of Cr_2O_3 addition on corrosion mechanism of refractory castables for waste melting furnaces and concurrent formation of hexavalent chromium. *Ceram. Int.* **2018**, *44*, 2383–2389. [CrossRef]
10. Heikal, M.; Radwan, M.M.; Al-Duaij, O.K. Physico-mechanical characteristics and durability of calcium aluminate blended cement subject to different aggressive media. *Constr. Build. Mater.* **2015**, *78*, 379–385. [CrossRef]
11. Verbinnen, B.; Billen, P.; Coninckxloo, M.V.; Vandecasteele, C. Heating temperature dependence of Cr(III) oxidation in the presence of alkali and alkaline earth salts and subsequent Cr(VI) leaching behavior. *Environ. Sci. Technol.* **2013**, *47*, 5858–5863. [CrossRef]
12. Garcia-Ramos, E.; Romero-Serrano, A.; Zeifert, B.; Flores-Sanchez, P.; Hallen-Lopez, M.; Palacios, E.G. Immobilization of chromium in slags using MgO and Al_2O_3. *Steel. Res. Int.* **2008**, *79*, 332–339. [CrossRef]

13. Mao, L.; Gao, B.; Deng, N.; Liu, L.; Cui, H. Oxidation behavior of Cr(III) during thermal treatment of chromium hydroxide in the presence of alkali and alkaline earth metal chlorides. *Chemosphere* **2016**, *145*, 1–9. [CrossRef] [PubMed]
14. Saha, R.; Nandi, R.; Saha, B. Sources and toxicity of hexavalent chromium. *J. Coord. Chem.* **2011**, *64*, 1782–1806. [CrossRef]
15. Bishop, M.E.; Glasser, P.; Dong, H.; Arey, B.; Kovarik, L. Reduction and immobilization of hexavalent chromium by microbially reduced Fe-bearing clay minerals. *Geochim. Et Cosmochim. Acta* **2014**, *133*, 186–203. [CrossRef]
16. Lee, Y.; Nassaralla, C.L. Minimization of hexavalent chromium in magnesite-chrome refractory. *Met. Mater. Trans. A* **1997**, *28*, 855–859. [CrossRef]
17. Chen, J.; Jiao, F.; Zhang, L.; Yao, H.; Ninomiya, Y. Elucidating the mechanism of Cr(VI) formation upon the interaction with metal oxides during coal oxy-fuel combustion. *J. Hazar. Mater.* **2013**, *261*, 260–268. [CrossRef] [PubMed]
18. Xu, T.; Nath, M.; Xu, Y.; Li, Y.; Liao, N.; Sang, S. Thermal evolution of Al_2O_3–CaO–Cr_2O_3 castables in different atmospheres. *Ceram. Int.* **2021**, *47*, 11043–11051. [CrossRef]
19. Mao, L.; Deng, N.; Liu, L.; Cui, H.; Zhang, W. Effects of Al_2O_3, Fe_2O_3, SiO_2 on Cr(VI) formation during heating of solid waste containing Cr(III). *Chem. Eng. J.* **2016**, *304*, 216–222. [CrossRef]
20. Nath, M.; Song, S.; Xu, T.; Wu, Y.; Li, Y. Effective inhibition of Cr(VI) in the Al_2O_3-CaO-Cr_2O_3 refractory castables system through silica gel assisted in-situ secondary phase tuning. *J. Clean Prod.* **2019**, *233*, 1038–1046. [CrossRef]
21. Mao, L.; Deng, N.; Liu, L.; Cui, H.; Zhang, W. Inhibition of Cr(III) oxidation during thermal treatment of simulated tannery sludge: The role of phosphate. *Chem. Eng. J.* **2016**, *294*, 1–8. [CrossRef]
22. Lin, S.H.; Chen, C.N.; Juang, R.S. Structure and thermal stability of toxic chromium(VI) species doped onto TiO_2 powders through heat treatment. *J. Environ. Manag.* **2009**, *90*, 1950–1955. [CrossRef] [PubMed]
23. Martinez, A.G.T.; Luz, A.P.; Braulio, M.A.L.; Pandolfelli, V.C. Creep behavior modeling of silica fume containing Al_2O_3-MgO refractory castables. *Ceram. Int.* **2012**, *38*, 327–332. [CrossRef]
24. Bie, C.; Sang, S.; Li, Y.; Xu, Y.; Qiao, J.; Fang, M. Effects of firing and operating atmospheres on microstructure and properties of phosphate bonded Cr_2O_3-Al_2O_3-ZrO_2 bricks. *China's Refract.* **2015**, *49*, 168–174.
25. Wu, Y.; Song, S.; Garbers-Craig, A.M.; Xue, Z. Formation and leachability of hexavalent chromium in the Al_2O_3-CaO-MgO-Cr_2O_3 system. *J. Eur. Ceram. Soc.* **2018**, *38*, 2649–2661. [CrossRef]
26. Liu, H.; Song, S.; Garbers-Craig, A.M.; Xue, Z. High-temperature stability of $Mg(Al,Cr)_2O_4$ spinel co-existing with calcium aluminates in air. *Ceram. Int.* **2019**, *45*, 16166–16172. [CrossRef]
27. Klyucharov, Y.V.; Eger, V.G. On the reaction between magnesiochromite and calcium oxide. *Refractories* **1963**, *4*, 137–144. [CrossRef]
28. Wu, Y.; Song, S.; Xue, Z.; Nath, M. Effect of temperature on hexavalent chromium formation in $(Al,Cr)_2O_3$ with calcium aluminate cement in air. *ISIJ Int.* **2019**, *59*, 1178–1183. [CrossRef]
29. Nath, M.; Song, S.; Garbers-Craig, A.M.; Li, Y. Phase evolution with temperature in chromium-containing refractory castables used for waste melting furnaces and Cr(VI) leachability. *Ceram. Int.* **2018**, *44*, 20391–20398. [CrossRef]
30. Nath, M.; Liao, N.; Xu, T.; Xu, Y.; Wu, Y.; Song, S.; Li, Y. Recent research on Cr-containing refractory castables. *Refract. Worldforum* **2021**, *13*, 48–57.
31. Nath, M.; Ghosh, A.; Tripathi, H.S. Hot corrosion behaviour of Al_2O_3–Cr_2O_3 refractory by molten glass at 1200 °C under static condition. *Corros. Sci.* **2016**, *102*, 153–160. [CrossRef]
32. Nath, M.; Kumar, P.; Song, S.; Li, Y.; Tripathi, H.S. Thermo-mechanical stability of bulk $(Al_{1-x}Cr_x)_2O_3$ solid solution. *Ceram. Int.* **2019**, *45*, 12411–12416. [CrossRef]
33. Nath, M.; Dana, K.; Gupta, S.; Tripathi, H.S. Hot corrosion behavior of slip-cast alumina-chrome refractory crucible against molten glass. *Mater. Corros.* **2014**, *65*, 742–747. [CrossRef]
34. Toxicological Review of Hexavalent Chromium. In *CAS No. 18540-29-9*; EPA: Washington, DC, USA, 1998.